Variational formulations for functionally graded nonlocal Bernoulli–Euler nanobeams

Raffaele Barretta [a], Luciano Feo [b], Raimondo Luciano [c,*], Francesco Marotti de Sciarra [a]

[a] Department of Structures for Engineering and Architecture, via Claudio 25, 80121 Naples, Italy
[b] Department of Civil Engineering, University of Salerno, 84084 Fisciano (Sa), Italy
[c] Department of Civil and Mechanical Engineering, University of Cassino and Southern Lazio, via G. Di Biasio 43, 03043 Cassino (FR), Italy

A B S T R A C T

The bending problem of functionally graded Bernoulli–Euler nanobeams is analyzed starting from a nonlocal thermodynamic approach and new nonlocal models are proposed. Nonlocal expressions of the free energy are presented, the variational formulations are then consistently provided and the differential equations with the associated higher-order boundary conditions are derived. Nonlocal Eringen and gradient elasticity constitutive models are recovered by specializing the variational scheme. Examples of nanobeams are explicitly carried out, detecting thus also new benchmarks for computational mechanics.

1. Introduction

Many studies have been delivered in recent years to define nonlocal models which are able to capture the effects of small length scale [1–12]. In the framework of nonlocal continuum mechanics [13–22] the long range forces between atoms and internal length scales have been introduced into the model by suitable modifications of the constitutive relations.

The theory of nonlocal continuum mechanics introduced by Eringen [23,24] has been used by Peddieson et al. [25] to provide a simple nonlocal Bernoulli–Euler beam model. Alternative constitutive proposals, also with reference to functionally graded materials, have been considered in several papers [26–35]. In particular, the gradient elasticity model has been addressed in [36] and the nonlocal elasticity model on the Timoshenko beam theory [37] has been formulated in many papers, see e.g. [38–43]. Recent exact solutions of functionally graded beams and plates have been contributed in [44–48]. Composite structures are effectively analyzed by resorting to experimental and numerical techniques in [49–63].

In nano- and micro-electromechanical systems (MEMS and NEMS), the actuator can be modeled as a Bernoulli–Euler nanocantilever subjected to a transverse point load at its tip. If the Eringen approach is considered for the nonlocal problem, the solution of the nonlocal beam coincides with the one of the classical (local) beam. Such a problem is overpassed by using gradient elasticity models and couple stress theories, see e.g. [2,8,36,64].

In this paper, following a thermodynamic approach [65–67], new nonlocal elastic models for bending of Bernoulli–Euler nanobeams, with Young modulus functionally graded in the cross-section, are provided starting from suitable definitions of the free energy which depends on a small length-scale parameter and a participation factor.

An advantage of the presented methodology consists in the fact that a nonlocal model can be formulated by the definition of the free energy so that a multitude of nonlocal models can be generated depending on the problem at hand.

Then nonlocal thermodynamics permits to build up a reliable methodology to stem the related variational formulation. As a consequence, the differential relations with the relevant boundary conditions can be obtained in a straightforward manner. Appropriate choices of the participation factor, entering in the nonlocal models, can make the nanobeam flexible or stiffer.

Simply supported nanobeams, clamped nanobeams and nanocantilevers are considered in order to investigate the influence of the nonlocal parameters. A comparison among the proposed models, the Eringen theory and the gradient elasticity model is thus performed.

2. Preliminary notions

A Bernoulli–Euler straight nanobeam occupying a domain B of a three-dimensional Euclidean space is considered. Let us assume that the Young modulus E of longitudinal fibers is functionally

* Corresponding author.
E-mail addresses: rabarret@unina.it (R. Barretta), l.feo@unisa.it (L. Feo), luciano@unicas.it (R. Luciano), marotti@unina.it (F. Marotti de Sciarra).

The final version of this manuscript is available in COMPOSITES. PART B, ENGINEERING. doi.org/10.1016/j.compstruct.2015.03.033

graded in the cross-section domain Ω, with corresponding elastic center G. The nanobeam axis is indicated by x and the bending plane is defined by the Cartesian axes (x,y) originating at the left cross-section elastic center. The axis orthogonal to the bending plane is denoted by z. Cross-sectional area and the elastic moment of inertia about the z-axis are respectively denoted by A and $I_E = \int_\Omega E(y,z)y^2 dA$. The axes y and z are assumed to be principal viz. $\int_\Omega E(y,z)yz\, dA = 0$.

The displacement field of the nanobeam and the nonvanishing kinematically compatible axial deformation field are respectively given by

$$\begin{cases} s_x(x,y,z) = -v^{(1)}(x)y \\ s_y(x,y,z) = v(x) \\ s_z(x,y,z) = 0 \end{cases} \qquad \varepsilon(x,y,z) = -v^{(2)}(x)y \tag{1}$$

where v is the transverse displacement along the y-axis and the superscript $\cdot^{(n)}$ denotes the nth derivative along the nanobeam axis x. The nanobeam bending curvature is $\chi = v^{(2)}$.

3. Variational formulations for nonlocal elastic models

Within the thermodynamic framework, a nonlocal model can be defined by introducing the Helmholtz free energy so that the complexity of a model is directly determined by the expression of the Helmholtz free energy and by the involved state variables.

Accordingly three nonlocal models for nanobeams are considered by defining the following three expressions of the free energy ψ_i, with $i = \{1,2,3\}$

$$\begin{bmatrix} \psi_1(\varepsilon,\varepsilon^{(1)}) \\ \psi_2(\varepsilon,\varepsilon^{(1)}) \\ \psi_3(\varepsilon,\varepsilon^{(1)}) \end{bmatrix} = \frac{1}{2}E\varepsilon^2 \begin{bmatrix} 1 \\ 1 \\ 1 \end{bmatrix} + \frac{1}{2}E\varepsilon^{(1)2} \begin{bmatrix} c^2 \\ \alpha^2 c^2 \\ \alpha^2 c^2 \end{bmatrix} + \frac{q}{A}\chi(\varepsilon) \begin{bmatrix} \alpha c^2 \\ c^2 \\ c^2 \end{bmatrix} + \frac{q^{(1)}}{A}\chi^{(1)}(\varepsilon^{(1)}) \begin{bmatrix} 0 \\ 0 \\ \alpha^2 c^4 \end{bmatrix}. \tag{2}$$

The link between the proposed models and existing theories will be clarified in the sequel.

The Young modulus of the material is E, the length-scale parameter is $c = e_0 l$ where l is the material length scale and e_0 represents a material constant [68]. The dimensionless parameter α acts as a participation factor so that the nonlocal models depend on two nonlocal parameters c and α. The mechanical meaning of the parameter α will be clarified in the sequel.

In this paper the coupled nonlocal models for nanobeams following from the free energies ψ_1, ψ_2 and ψ_3 will be denoted by $C1$, $C2$ and $C3$.

The nonlocal first principle of thermodynamic is written in a global form and the second principle is expressed in its usual local form [66,67] so that the vanishing of the body energy dissipation in a nonlocal elastic model can be expressed as follows

$$\int_B \bar{\sigma}\dot{\varepsilon} dV = \int_B \dot{\psi}_i dV, \quad i = \{1,2,3\} \tag{3}$$

where ψ_i is the Helmholtz free energy of the nanobeam and $\bar{\sigma}$ is the nonlocal axial stress. The superscript dot denotes differentiation with respect to the time.

Once a definition of the free energy is given, the related nonlocal model for nanobeams can be reliably derived in a nonlocal variational form and, as a consequence, the corresponding differential relations with the required boundary conditions can be consistently derived.

In fact substituting the time derivative of the free energies (2) into Eq. (3) we get the relations

$$\int_B \bar{\sigma}\dot{\varepsilon} \begin{bmatrix} 1 \\ 1 \\ 1 \end{bmatrix} dV = \int_B \left(E\varepsilon\dot{\varepsilon} \begin{bmatrix} 1 \\ 1 \\ 1 \end{bmatrix} + E\varepsilon^{(1)}\dot{\varepsilon}^{(1)} \begin{bmatrix} c^2 \\ \alpha^2 c^2 \\ \alpha^2 c^2 \end{bmatrix} + \frac{q}{A}\partial_\varepsilon\chi(\varepsilon)\dot{\varepsilon} \begin{bmatrix} \alpha c^2 \\ c^2 \\ c^2 \end{bmatrix} + \frac{q^{(1)}}{A}\partial_{\varepsilon^{(1)}}\chi^{(1)}(\varepsilon^{(1)})\dot{\varepsilon}^{(1)} \begin{bmatrix} 0 \\ 0 \\ \alpha^2 c^4 \end{bmatrix} \right) dV, \tag{4}$$

where $\partial_\blacksquare$ is the derivative with respect to the variable $\blacksquare$, so that, using the kinematically compatible deformation field $(1)_2$, the following variational formulations are obtained for the considered three coupled models

$$\int_0^L M\dot{v}^{(2)} dx \begin{bmatrix} 1 \\ 1 \\ 1 \end{bmatrix} = \int_0^L M_0\dot{v}^{(2)} dx \begin{bmatrix} 1 \\ 1 \\ 1 \end{bmatrix} + \int_0^L q\dot{v}^{(2)} dx \begin{bmatrix} \alpha c^2 \\ c^2 \\ c^2 \end{bmatrix} + \int_0^L M_1\dot{v}^{(3)} dx \begin{bmatrix} c^2 \\ \alpha^2 c^2 \\ \alpha^2 c^2 \end{bmatrix} + \int_0^L q^{(1)}\dot{v}^{(3)} dx \begin{bmatrix} 0 \\ 0 \\ \alpha^2 c^4 \end{bmatrix} \tag{5}$$

where the stress resultant moments are given by

$$(M, M_0, M_1) = -\int_\Omega (\bar{\sigma}, \sigma_0, \sigma_1) y dA = -\int_\Omega (\bar{\sigma}, E\varepsilon, E\varepsilon^{(1)}) y dA. \tag{6}$$

3.1. Governing equations and boundary conditions for nonlocal elastic models

Integrating by parts Eq. (5) the following differential relations for the nonlocal coupled models are provided

$$M^{(2)} \begin{bmatrix} 1 \\ 1 \\ 1 \end{bmatrix} - q^{(2)} \begin{bmatrix} \alpha c^2 \\ c^2 \\ c^2 \end{bmatrix} + q^{(4)} \begin{bmatrix} 0 \\ 0 \\ \alpha^2 c^4 \end{bmatrix} = M_0^{(2)} \begin{bmatrix} 1 \\ 1 \\ 1 \end{bmatrix} - M_1^{(3)} \begin{bmatrix} c^2 \\ \alpha^2 c^2 \\ \alpha^2 c^2 \end{bmatrix} \tag{7}$$

where the corresponding consistent boundary conditions are reported in Table 1.

The classical differential relationship between bending moment and applied load is recovered for the nonlocal coupled models $C1$, $C2$ and $C3$ by considering the l.h.s. of Eq. (3). Replacing $\dot{\varepsilon}$ by using the kinematically compatible relation in Eq. $(1)_2$ and integrating by parts we get

$$M^{(2)} = q. \tag{8}$$

The boundary conditions at $x = \{0, L\}$ provide the conditions $T = -M^{(1)} = F$ and $M = \mathcal{M}$ where T is the shear force, q is the distributed transverse load and $(F, \mathcal{M})$ are the transverse force and couple respectively.

Then the nonlocal elastic equilibrium equation for nanobeams associated with the considered models can be provided by expressing the differential Eq. (7) in terms of the transverse displacement v using Eq. $(1)_2$ and (6). In fact, remarking the equalities

$$(M_0, M_1) = -\int_\Omega (E\varepsilon, E\varepsilon^{(1)}) y dA = (I_E v^{(2)}, I_E v^{(3)}), \tag{9}$$

the governing differential equations for the bending of the nonlocal Bernoulli–Euler nanobeam under distributed transverse loads are

$$I_E v^{(6)} \begin{bmatrix} c^2 \\ \alpha^2 c^2 \\ \alpha^2 c^2 \end{bmatrix} - I_E v^{(4)} \begin{bmatrix} 1 \\ 1 \\ 1 \end{bmatrix} = -q \begin{bmatrix} 1 \\ 1 \\ 1 \end{bmatrix} + q^{(2)} \begin{bmatrix} \alpha c^2 \\ c^2 \\ c^2 \end{bmatrix} - q^{(4)} \begin{bmatrix} 0 \\ 0 \\ \alpha^2 c^4 \end{bmatrix} \tag{10}$$

The final version of this manuscript is available in COMPOSITES. PART B, ENGINEERING. doi.org/10.1016/j.compstruct.2015.03.033

Table 1
Boundary conditions pertaining to the coupled nanobeam models.

Nonlocal model	Kinematic boundary conditions	Static boundary conditions
(C1) (C2) (C3)	v	$-M^{(1)}\begin{bmatrix}1\\1\\1\end{bmatrix}+q^{(1)}\begin{bmatrix}\alpha c^2\\c^2\\c^2\end{bmatrix}-q^{(3)}\begin{bmatrix}0\\0\\\alpha^2c^4\end{bmatrix}=-M_0^{(1)}\begin{bmatrix}1\\1\\1\end{bmatrix}+M_1^{(2)}\begin{bmatrix}c^2\\\alpha^2c^2\\\alpha^2c^2\end{bmatrix}$
(C1) (C2) (C3)	$v^{(1)}$	$M\begin{bmatrix}1\\1\\1\end{bmatrix}-q\begin{bmatrix}\alpha c^2\\c^2\\c^2\end{bmatrix}+q^{(2)}\begin{bmatrix}0\\0\\\alpha^2c^4\end{bmatrix}=M_0\begin{bmatrix}1\\1\\1\end{bmatrix}-M_1^{(1)}\begin{bmatrix}c^2\\\alpha^2c^2\\\alpha^2c^2\end{bmatrix}$
(C1) (C2) (C3)	$v^{(2)}$	$-q^{(1)}\begin{bmatrix}0\\0\\\alpha^2c^4\end{bmatrix}=M_1\begin{bmatrix}c^2\\\alpha^2c^2\\\alpha^2c^2\end{bmatrix}$

Table 2
Boundary conditions in terms of transverse displacement for nonlocal nanobeams.

Nonlocal Model	Kinematic boundary conditions	Static boundary conditions
(C1) (C2) (C3)	v	$-I_E v^{(3)}\begin{bmatrix}1\\1\\1\end{bmatrix}+I_E v^{(5)}\begin{bmatrix}c^2\\\alpha^2c^2\\\alpha^2c^2\end{bmatrix}=T\begin{bmatrix}1\\1\\1\end{bmatrix}+q^{(1)}\begin{bmatrix}\alpha c^2\\c^2\\c^2\end{bmatrix}-q^{(3)}\begin{bmatrix}0\\0\\\alpha^2c^4\end{bmatrix}$
(C1) (C2) (C3)	$v^{(1)}$	$I_E v^{(2)}\begin{bmatrix}1\\1\\1\end{bmatrix}-I_E v^{(4)}\begin{bmatrix}c^2\\\alpha^2c^2\\\alpha^2c^2\end{bmatrix}=M\begin{bmatrix}1\\1\\1\end{bmatrix}-q\begin{bmatrix}\alpha c^2\\c^2\\c^2\end{bmatrix}+q^{(2)}\begin{bmatrix}0\\0\\\alpha^2c^4\end{bmatrix}$
(C1) (C2) (C3)	$v^{(2)}$	$I_E v^{(3)}\begin{bmatrix}c^2\\\alpha^2c^2\\\alpha^2c^2\end{bmatrix}=-q^{(1)}\begin{bmatrix}0\\0\\\alpha^2c^4\end{bmatrix}$

the related boundary conditions follow from Table 1 and are reported in Table 2.

The expression of the bending moment for the considered coupled models can be recovered from the related variational formulations (5) by noting the equalities (A.3) reported in Appendix A.

Hence we get

$$M\begin{bmatrix}1\\1\\1\end{bmatrix}=M_0\begin{bmatrix}1\\1\\1\end{bmatrix}-M_1^{(1)}\begin{bmatrix}c^2\\\alpha^2c^2\\\alpha^2c^2\end{bmatrix}+q\begin{bmatrix}\alpha c^2\\c^2\\c^2\end{bmatrix}-q^{(2)}\begin{bmatrix}0\\0\\\alpha^2c^4\end{bmatrix} \tag{11}$$

which can be rewritten in terms of displacements as

$$M\begin{bmatrix}1\\1\\1\end{bmatrix}=I_E v^{(2)}\begin{bmatrix}1\\1\\1\end{bmatrix}-I_E v^{(4)}\begin{bmatrix}c^2\\\alpha^2c^2\\\alpha^2c^2\end{bmatrix}+q\begin{bmatrix}\alpha c^2\\c^2\\c^2\end{bmatrix}-q^{(2)}\begin{bmatrix}0\\0\\\alpha^2c^4\end{bmatrix}. \tag{12}$$

Remark 3.1. If $\alpha=0$, the coupled model $C1$ provides the gradient elasticity model (GM) for Bernoulli–Euler nanobeams, see [36,43] for Timoshenko nanobeams. Moreover, if $\alpha=0$, the coupled models $C2$ and $C3$ coincide and they reduce to the Eringen model (EM), see [24].

A nonvanishing value of the participation factor α determines the coupling between the Eringen and gradient nonlocal models in the considered coupled models $C1$, $C2$ and $C3$.

If $\alpha=1$, the coupled models $C1$ and $C2$ coincide for any value of c and a pure coupling between the Eringen and gradient models is recovered.

The relationship among these models are summarized in Table 3. Note that, if the applied load is uniform, the models $C2$ and $C3$ are coincident for any value of α.

Remark 3.2. Eq. (5) of the variational formulations for the considered coupled models allow us to derive in a straightforward manner the bilinear form of the elastic energy associated with the models $C1$, $C2$ and $C3$ as reported in a forthcoming paper. For sake of completeness, the expressions of the bilinear forms of the elastic energy are reported in the next Table 4 in order to show that they are symmetric and positive for any value of the length-scale parameter c and of the participation factor α.

Note that the participation factor α does not enter in the expression of $a(v,v)$ of the model $C1$ as opposed to the expressions pertaining to the models $C2$ and $C3$. The model $C1$ provides the possibility of stiffening or softening the nanobeam in a wider range than the models $C2$ and $C3$ as shown in Section 5.

4. Closed form analytical solutions in bending problems

In order to show the effectiveness of the models, the following three examples are considered: (i) simply supported nanobeam

Table 3
Comparison among different nonlocal models in terms of the participation factor α.

Nonlocal model	Participation factor α	
	0	1
C1	GM	C2
C2	C3, EM	C1
C3	C2, EM	

Table 4
Bilinear forms of the elastic energy for the coupled nonlocal models.

Nonlocal Model	Bilinear forms of the elastic energy $a(v,v)$
C1	$\int_0^L I_E v^{(2)} v^{(2)}dx+c^2\int_0^L I_E v^{(3)} v^{(3)}dx$
C2	$\int_0^L I_E v^{(2)} v^{(2)}dx+\alpha^2c^2\int_0^L I_E v^{(3)} v^{(3)}dx$
C3	$\int_0^L I_E v^{(2)} v^{(2)}dx+\alpha^2c^2\int_0^L I_E v^{(3)} v^{(3)}dx$

The final version of this manuscript is available in COMPOSITES. PART B, ENGINEERING. doi.org/10.1016/j.compstruct.2015.03.033

subjected to a parabolic distributed load; (ii) clamped nanobeam subjected to a parabolic distributed load; (iii) nanocantilever subjected to a linearly distributed load.

4.1. Simply supported nanobeam subjected to a parabolic distributed load

A simply supported nanobeam with length L is subjected to a parabolic distributed load $q(x) = 4a(-x^2/L^2 + x/L)$ where a is the value of the distributed load at the nanobeam midpoint.

The nonlocal differential equations of the considered coupled models follow from Eq. (10) and are given by

$$I_E v^{(6)} \begin{bmatrix} c^2 \\ \alpha^2 c^2 \\ \alpha^2 c^2 \end{bmatrix} - I_E v^{(4)} \begin{bmatrix} 1 \\ 1 \\ 1 \end{bmatrix} = -q \begin{bmatrix} 1 \\ 1 \\ 1 \end{bmatrix} + q^{(2)} \begin{bmatrix} \alpha^2 c^2 \\ c^2 \\ c^2 \end{bmatrix} \tag{13}$$

where the six boundary conditions are

$$\begin{cases} v(0)\begin{bmatrix} 1 \\ 1 \\ 1 \end{bmatrix} = \begin{bmatrix} 0 \\ 0 \\ 0 \end{bmatrix}, \; I_E v^{(2)}(0)\begin{bmatrix} 1 \\ 1 \\ 1 \end{bmatrix} - I_E v^{(4)}(0)\begin{bmatrix} c^2 \\ \alpha^2 c^2 \\ \alpha^2 c^2 \end{bmatrix} = -q(0)\begin{bmatrix} \alpha^2 c^2 \\ c^2 \\ c^2 \end{bmatrix} + q^{(2)}(0)\begin{bmatrix} 0 \\ 0 \\ \alpha^2 c^4 \end{bmatrix}, \\ \qquad I_E v^{(3)}(0)\begin{bmatrix} 1 \\ 1 \\ 1 \end{bmatrix} = -q^{(1)}(0)\begin{bmatrix} 0 \\ 0 \\ c^2 \end{bmatrix}, I_E v^{(3)}(L)\begin{bmatrix} 1 \\ 1 \\ 1 \end{bmatrix} = -q^{(1)}(L)\begin{bmatrix} 0 \\ 0 \\ c^2 \end{bmatrix} \\ v(L)\begin{bmatrix} 1 \\ 1 \\ 1 \end{bmatrix} = \begin{bmatrix} 0 \\ 0 \\ 0 \end{bmatrix}, I_E v^{(2)}(L)\begin{bmatrix} 1 \\ 1 \\ 1 \end{bmatrix} - I_E v^{(4)}(L)\begin{bmatrix} c^2 \\ \alpha^2 c^2 \\ \alpha^2 c^2 \end{bmatrix} = -q(L)\begin{bmatrix} \alpha^2 c^2 \\ c^2 \\ c^2 \end{bmatrix} + q^{(2)}(L)\begin{bmatrix} 0 \\ 0 \\ \alpha^2 c^4 \end{bmatrix}. \end{cases} \tag{14}$$

The models $C1$ and $C2$ coincide if the participation factor is set equal to one and the model $C3$ is different from model $C2$ due to the presence of the derivatives $q^{(1)}$ and $q^{(2)}$ of the applied load in the differential Eq. (13) and in the boundary conditions (14).

The transverse displacement fields of the coupled models are then given in the following form

$$\begin{cases} (C1) \quad v_1(x) = v_{\mathcal{L}}(x) + \frac{\alpha c^3(1+e^{\frac{L}{c}})(L^2+12c^2(-1+\alpha))}{3(-1+e^{\frac{L}{c}})I_E L} - \frac{12c^2\alpha x^3(-1+\alpha)}{18I_E L} + \frac{\alpha x\left(-120c^4(-1+\alpha)+10c^2L^2(-1+\alpha)\right)}{30I_E L} \\ + \frac{\frac{\alpha c^3 e^{\frac{L}{c}} L(L^2+12c^2(-1+\alpha))}{-1+e^{\frac{L}{c}}} - \frac{\alpha c^3 e^{\frac{L}{c}} L(L^2+12c^2(-1+\alpha))}{-1+e^{\frac{L}{c}}} + \alpha c^2 x^4(-1+\alpha)}{3I_E L^2} + \frac{4\alpha c^4 x^2(-1+\alpha)}{I_E L^2} \\ (C2) \quad v_2(x) = v_{\mathcal{L}}(x) - \frac{4\alpha c^4 x^2 x^2(-1+x^2)}{I_E L^2} + \frac{12c^2\alpha x^3(-1+x^2)}{18I_E L} - \frac{\alpha c^3\left(1+e^{\frac{L}{c}}\right)x^3\left(-L^2+12c^2(-1+x^2)\right)}{3(-1+e^{\frac{L}{c}})I_E L} \\ + \frac{\alpha x\left(-10c^2L^2(-1+x^2)+120c^4x^2(-1+x^2)\right)}{30I_E L} - \frac{\alpha c^2 x^4(-1+x^2)}{3I_E L^2} + \frac{\frac{3c^4 e^{\frac{L}{c}} L x^4(12\alpha c^2+\alpha L^2-12\alpha c^2 x^2)}{3\alpha-3\alpha e^{\frac{L}{c}} x} + \frac{\alpha c^3 e^{\frac{L}{c}} L x^3(-L^2+12c^2(-1+x^2))}{-1+e^{\frac{L}{c}}}}{3I_E L^2} \\ (C3) \quad v_3(x) = v_{\mathcal{L}}(x) - \frac{4\alpha c^4 x^2 x^4}{I_E L^2} - \frac{\alpha c^3(1+e^{\frac{L}{c}})x^3(-L^2+12c^2x^2)}{3(-1+e^{\frac{L}{c}})I_E L} + \frac{12c^2\alpha x^3(-1+x^2)}{18I_E L} + \frac{\alpha x(120c^4x^4-10c^2L^2(-1+x^2))}{30I_E L} \\ + \frac{-\alpha c^2 x^4(-1+x^2) - \frac{\alpha c^3 e^{\frac{L}{c}} L x^3(L^2-12c^2x^2)}{-1+e^{\frac{L}{c}}} + \frac{3c^3 e^{\frac{L}{c}} L^2 x^3(\alpha L^2-12\alpha c^2 x^2)}{3L-3e^{\frac{L}{c}} L}}{3I_E L^2} \end{cases} \tag{15}$$

where $v_{\mathcal{L}}$ is the classical (local) transverse displacement

$$v_{\mathcal{L}}(x) = \frac{aL^3 x}{30I_E} - \frac{aLx^3}{18I_E} + \frac{ax^5}{30I_E L} - \frac{ax^6}{90I_E L^2}. \tag{16}$$

The transverse displacement fields v_1, v_2 and v_3 reduce to the classical (local) one $v_{\mathcal{L}}$ for $c = 0$ and are not bounded for the length-scale parameter $c \to +\infty$.

The limit displacements of the models $C2$ and $C3$ for $\alpha \to +\infty$ can be easily evaluated and, in terms of the length-scale parameter c, are given by $v_{2\infty}(x) = a(10c^2 + L^2)(L - x)x/30I_E$ and $v_{3\infty}(x) = a(L - x)x(L^4 + 10c^2(L^2 + Lx - x^2))/30I_E L^2$. On the contrary, the displacements of the model $C1$ are not bounded for $\alpha \to \pm\infty$.

4.2. Clamped nanobeam subjected to a parabolic distributed load

A clamped nanobeam with length L is subjected to a parabolic distributed load $q(x) = 4a(-x^2/L^2 + x/L)$ where a is the value of the distributed load at the nanobeam midpoint.

The nonlocal differential equations of the considered coupled models follow from Eq. (10) and are given by

$$I_E v^{(6)} \begin{bmatrix} c^2 \\ \alpha^2 c^2 \\ \alpha^2 c^2 \end{bmatrix} - I_E v^{(4)} \begin{bmatrix} 1 \\ 1 \\ 1 \end{bmatrix} = -q \begin{bmatrix} 1 \\ 1 \\ 1 \end{bmatrix} + q^{(2)} \begin{bmatrix} \alpha^2 c^2 \\ c^2 \\ c^2 \end{bmatrix} \tag{17}$$

where the six boundary conditions are

$$\begin{cases} v(0)\begin{bmatrix} 1 \\ 1 \\ 1 \end{bmatrix} = \begin{bmatrix} 0 \\ 0 \\ 0 \end{bmatrix}, \; v^{(1)}(0)\begin{bmatrix} 1 \\ 1 \\ 1 \end{bmatrix} = \begin{bmatrix} 0 \\ 0 \\ 0 \end{bmatrix}, \; I_E v^{(3)}(0)\begin{bmatrix} 1 \\ 1 \\ 1 \end{bmatrix} = -q^{(1)}(0)\begin{bmatrix} 0 \\ 0 \\ c^2 \end{bmatrix} \\ v(L)\begin{bmatrix} 1 \\ 1 \\ 1 \end{bmatrix} = \begin{bmatrix} 0 \\ 0 \\ 0 \end{bmatrix}, \; v^{(1)}(L)\begin{bmatrix} 1 \\ 1 \\ 1 \end{bmatrix} = \begin{bmatrix} 0 \\ 0 \\ 0 \end{bmatrix}, \; I_E v^{(3)}(L)\begin{bmatrix} 1 \\ 1 \\ 1 \end{bmatrix} = -q^{(1)}(L)\begin{bmatrix} 0 \\ 0 \\ c^2 \end{bmatrix} \end{cases} \tag{18}$$

The models $C1$ and $C2$ coincide if the participation factor is set equal to one and the model $C3$ does not match model $C2$ due to the presence of the derivatives $q^{(1)}$ and $q^{(2)}$ of the applied load in the differential equations and in the boundary conditions.

The final version of this manuscript is available in COMPOSITES. PART B, ENGINEERING. doi.org/10.1016/j.compstruct.2015.03.033

The transverse displacement fields of the coupled models are then given in the following form

$$
\begin{cases}
(C1) \quad v_1(x) = v_{\mathcal{L}}(x) + \frac{ac^2 e^{-\frac{L}{c}}}{3(-1+e^{\frac{L}{c}})l_E L^2} \\
\Big[c(e^{\frac{L}{c}}-e^{\frac{L}{c}})(-1+e^{\frac{L}{c}})L^3 + 12c^3(e^{\frac{L}{c}}-e^{\frac{L}{c}})(-1+e^{\frac{L}{c}})L(-1+\alpha) + 12c^2 e^{\frac{L}{c}}(-1+e^{\frac{L}{c}})x(-L+x)(-1+\alpha) \\
+e^{\frac{L}{c}}(-1+e^{\frac{L}{c}})x(-L+x)(L^2+x^2(-1+\alpha)+L(x-x\alpha))\Big] \\
(C2) \quad v_2(x) = v_{\mathcal{L}}(x) + \frac{ac^2 e^{-\frac{L}{c\alpha}}}{3(-1+e^{\frac{L}{c\alpha}})l_E L^2} \\
\Big[ce^{\frac{L}{c\alpha}}L\alpha^3(-L^2+12c^2(-1+\alpha^2)) + ce^{\frac{2L}{c\alpha}}L\alpha^3(-L^2+12c^2(-1+\alpha^2)) + e^{\frac{L+x}{c\alpha}}(L^2x^2+L^3\alpha^2(-x+c\alpha)-x^2(-1+\alpha^2)(x^2+12c^2\alpha^2) \\
+2L(-1+\alpha^2)(x^3+6c^2x\alpha^2-6c^3\alpha^3)) + e^{\frac{L}{c\alpha}}(-L^2x^2+L^3\alpha^2(x+c\alpha)+x^2(-1+\alpha^2)(x^2+12c^2\alpha^2)-2L(-1+\alpha^2)(x^3+6c^2x\alpha^2+6c^3\alpha^3))\Big] \\
(C3) \quad v_3(x) = v_{\mathcal{L}}(x) + \frac{ac^2 e^{-\frac{L}{c}}}{3(-1+e^{\frac{L}{c}})l_E L^2} \\
\Big[ce^{\frac{L}{c}}L\alpha^3(-L^2+12c^2\alpha^2) + ce^{\frac{2L}{c}}L\alpha^3(-L^2+12c^2\alpha^2) + e^{\frac{L+x}{c}}(L^2x^2-12c^2x^2\alpha^4+L^3\alpha^2(-x+c\alpha)-x^4(-1+\alpha^2)+2L(6c^2x\alpha^4-6c^3\alpha^5 \\
+x^3(-1+\alpha^2))) + e^{\frac{L}{c}}(-L^2x^2+12c^2x^2\alpha^4+L^3\alpha^2(x+c\alpha)+x^4(-1+\alpha^2)-2L(6c^2x\alpha^4+6c^3\alpha^5+x^3(-1+\alpha^2)))\Big]
\end{cases}
\tag{19}
$$

where $v_{\mathcal{L}}$ is the classical (local) transverse displacement

$$
v_{\mathcal{L}}(x) = \frac{aL^2x^2}{30l_E} - \frac{aLx^3}{18l_E} + \frac{ax^5}{30l_E L} - \frac{ax^6}{90l_E L^2}. \tag{20}
$$

The transverse displacement fields v_1, v_2 and v_3 reduce to the classical (local) one $v_{\mathcal{L}}$ for $c = 0$ and $v_{\mathcal{L}}$ represents the lower bound of the nonlocal displacements.

Moreover, the upper bounds $v_{1\infty}$ and $v_{2\infty}$ of the displacement fields v_1 and v_2 can be obtained by evaluating the limit for $c \to +\infty$ and are given by

$$
\begin{aligned}
v_{1\infty}(x) &= \frac{a(L-x)^2x^2(L^2+2Lx-2x^2)\alpha}{180l_E L^2}, \\
v_{2\infty}(x) &= \frac{a(L-x)^2x^2(L^2+2Lx-2x^2)}{180l_E L^2\alpha^2}
\end{aligned}
\tag{21}
$$

and they depend on the participation factor α.

The limit displacements of the models $C2$ and $C3$ for $\alpha \to +\infty$ can be evaluated in terms of the length-scale parameter c and are given by $v_{2\infty}(x) = 0$ and $v_{3\infty}(x) = ac^2(L-x)^2x^2/3l_E L^2$.

On the contrary, the displacements of the model $C3$ are not bounded for $c \to +\infty$ and the displacements of the model $C1$ are not bounded for $\alpha \to \pm\infty$.

Hence the displacement fields v_1 and v_2 must belong to the strip limited by the functions $v_{\mathcal{L}}$ and $v_{1\infty}$, $v_{2\infty}$ (for a given α) respectively. On the contrary, the transverse displacement field v_3 is not bounded for the length-scale parameter $c \to +\infty$.

The bending moments of the coupled models are obtained by Eq. (12) and depend on the length-scale parameter c and the participation factor α.

In particular, the bending moment M of the coupled model $C1$ is given by $M_{C1} = M_{\mathcal{L}} + \frac{2}{3}ac^2\alpha$. The bending moments of the coupled models $C2$ and $C3$ coincide and are given by $M_{C2} = M_{C3} = M_{\mathcal{L}} + \frac{2}{3}ac^2$ where $M_{\mathcal{L}} = a(L^4 - 5L^3x + 10Lx^3 - 5x^4)/15L^2$ is the bending moment of the local model.

4.3. Nanocantilever subjected to a linearly distributed load

A nanocantilever with length L is subjected to a linearly distributed load $q(x) = a(1 - x/L)$ where a is the value of the distributed load at the cantilever cross-section $x = 0$.

The nonlocal differential equations of the considered coupled models follow from Eq. (10) and are given by

$$
I_E v^{(6)} \begin{bmatrix} c^2 \\ \alpha^2 c^2 \\ \alpha^2 c^2 \end{bmatrix} - I_E v^{(4)} \begin{bmatrix} 1 \\ 1 \\ 1 \end{bmatrix} = -q \begin{bmatrix} 1 \\ 1 \\ 1 \end{bmatrix} \tag{22}
$$

where the six boundary conditions are

$$
\begin{cases}
v(0)\begin{bmatrix}1\\1\\1\end{bmatrix} = \begin{bmatrix}0\\0\\0\end{bmatrix}, \quad v^{(1)}(0)\begin{bmatrix}1\\1\\1\end{bmatrix} = \begin{bmatrix}0\\0\\0\end{bmatrix}, \quad I_E v^{(3)}(0)\begin{bmatrix}c^2\\\alpha^2c^2\\\alpha^2c^2\end{bmatrix} = -q^{(1)}(0)\begin{bmatrix}0\\0\\\alpha^2c^4\end{bmatrix} \\
-I_E v^{(3)}(L)\begin{bmatrix}1\\1\\1\end{bmatrix} + I_E v^{(5)}(L)\begin{bmatrix}c^2\\\alpha^2c^2\\\alpha^2c^2\end{bmatrix} = q^{(1)}(L)\begin{bmatrix}\alpha c^2\\c^2\\c^2\end{bmatrix}, \\
I_E v^{(2)}(L)\begin{bmatrix}1\\1\\1\end{bmatrix} - I_E v^{(4)}(L)\begin{bmatrix}c^2\\\alpha^2c^2\\\alpha^2c^2\end{bmatrix} = -q(L)\begin{bmatrix}\alpha c^2\\c^2\\c^2\end{bmatrix}, \quad I_E v^{(3)}(L)\begin{bmatrix}c^2\\\alpha^2c^2\\\alpha^2c^2\end{bmatrix} = -q^{(1)}(L)\begin{bmatrix}0\\0\\\alpha^2c^4\end{bmatrix}
\end{cases}
\tag{23}
$$

According to Table 3, the models $C1$ and $C2$ coincide if the participation factor is equal to one. Note that the model $C3$ differs from model $C2$ due to the presence of the derivative $q^{(1)}$ of the applied load in the boundary conditions (23).

The transverse displacement fields of the coupled models are then given in the following form

$$
\begin{cases}
(C1) \quad v_1(x) = v_{\mathcal{L}}(x) - \frac{6c^2ax^2(-1+\alpha)}{12l_E} + \frac{2c^3ax^3(-1+\alpha)}{12l_E L} + \frac{ac^2x(-L^2+2c^2(-1+\alpha))}{2l_E L} \\
- \frac{ac^3e^{\frac{L}{c}}(L^2+2c^2(-1+e^{\frac{L}{c}})(-1+\alpha))}{2(-1+e^{\frac{2L}{c}})l_E L} + \frac{ac^3e^{\frac{L-x}{c}}(-e^{\frac{L}{c}}L^2+2c^2(-1+e^{\frac{L}{c}})(-1+\alpha))}{2(-1+e^{\frac{2L}{c}})l_E L} \\
- \frac{ac^3((-1-e^{\frac{2L}{c}})L^2+2c^2(-1+e^{\frac{L}{c}})^2(-1+\alpha))}{2(-1+e^{\frac{2L}{c}})l_E L} \\
(C2) \quad v_2(x) = v_{\mathcal{L}}(x) - \frac{2c^2ax^3(-1+\alpha^2)}{12l_E L} - \frac{ac^2x\alpha^2(L^2+2c^2(-1+\alpha^2))}{2l_E L} \\
+ \frac{6c^2ax^2(-1+\alpha^2)}{12l_E} + \frac{ac^3e^{\frac{L}{c\alpha}}x^3(-L^2+2c^2(-1+e^{\frac{L}{c\alpha}})(-1+\alpha^2))}{2(-1+e^{\frac{2L}{c\alpha}})l_E L} \\
- \frac{ac^3e^{\frac{L}{c\alpha}-\frac{L}{c}}x^3(e^{\frac{L}{c}}L^2+2c^2(-1+e^{\frac{L}{c\alpha}})(-1+\alpha^2))}{2(-1+e^{\frac{2L}{c\alpha}})l_E L} + \frac{ac^3x^3((1+e^{\frac{2L}{c\alpha}})L^2+2c^2(-1+e^{\frac{L}{c\alpha}})^2(-1+\alpha^2))}{2(-1+e^{\frac{2L}{c\alpha}})l_E L} \\
(C3) \quad v_3(x) = v_{\mathcal{L}}(x) - \frac{ac^2x\alpha^2(L^2+2c^2\alpha^2)}{2l_E L} + \frac{c^3e^{\frac{L}{c}}x^3(aL^2+2ac^2\alpha^2-2ac^2e^{\frac{L}{c}}\alpha^2)}{2l_E L-2e^{\frac{2L}{c}}l_E L} \\
+ \frac{ac^3x^3((1+e^{\frac{2L}{c}})L^2+2c^2(-1+e^{\frac{L}{c}})^2\alpha^2)}{2(-1+e^{\frac{2L}{c}})l_E L} - \frac{2c^2ax^3(-1+\alpha^2)}{12l_E L} + \frac{6c^2ax^2(-1+\alpha^2)}{12l_E} \\
- \frac{ac^3e^{\frac{L}{c}-\frac{L}{c\alpha}}x^3(-2c^2\alpha^2+e^{\frac{L}{c}}(L^2+2c^2\alpha^2))}{2(-1+e^{\frac{2L}{c}})l_E L}
\end{cases}
\tag{24}
$$

The final version of this manuscript is available in COMPOSITES. PART B, ENGINEERING. doi.org/10.1016/j.compstruct.2015.03.033

where v_C is the classical (local) transverse displacement

$$v_C(x) = \frac{aL^2x^2}{12I_E} - \frac{aLx^3}{12I_E} + \frac{ax^4}{24I_E} - \frac{ax^5}{120I_EL}. \tag{25}$$

The transverse displacement fields v_1, v_2 and v_3 reduce to the classical (local) one v_C for $c = 0$ and are not bounded for the scale parameter $c \to +\infty$.

The limit displacements for $\alpha \to +\infty$ of the models $C2$ and $C3$ can be easily evaluated and are given by $v_{2\infty}(x) = -a(12c^2 - L^2)x^2/48I_E$ and $v_{3\infty}(x) = ax^2(L^3 + 8c^2(-3L + x))/48I_EL$ in terms of the length-scale parameter c. On the contrary, the displacements of the model $C1$ are not bounded.

5. Numerical examples

As a special case, the coupled models $C1$, $C2$ and $C3$ are hereafter specialized to obtain nanobeam formulations based on the Eringen nonlocal elasticity theory (EM) and on the gradient elasticity model (GM).

Exact solutions of the benchmarks assessed in Section 4 are exploited to enlighten the effectiveness of the new nonlocal models in comparison with existing treatments.

For sake of convenience, we introduce the following dimensionless quantities

$$\xi = \frac{x}{L}, \quad \tau = \frac{c}{L}, \quad v_i^*(\xi) = v_i(x)\frac{I_E}{aL^4}, \tag{26}$$

with $i = \{1,2,3\}$, so that only the dimensionless length-scale parameter $\tau \in \{0, 0.1, 0.2, 0.3, 0.4, 0.5\}$ and the participation factor α are required in computations.

- The maximum dimensionless deflections v_1^*, v_2^* and v_3^* of the models $C1$, $C2$ and $C3$ for a simply supported nanobeam subjected to a parabolic distributed load is plotted in Fig. 1 for different values of the dimensionless length-scale parameter $\tau \in \{0, 0.1, 0.2, 0.3, 0.4, 0.5\}$. The participation factor α ranges in the interval $[-1, 2]$.

Setting $\alpha = 0$, the maximum dimensionless deflection obtained by the models $C2$ and $C3$ for a given τ coincides with the one evaluated by the Eringen model (EM). Further, for $\alpha = 0$, the maximum dimensionless deflection obtained by the model $C1$ coincides with the one calculated by the gradient elasticity model (GM). For $\alpha = 1$ the maximum dimensionless deflections obtained by models $C1$ and $C2$ matches. For $\tau = 0$ the nonlocal models degenerate to the local (L) one.

For a given dimensionless scale parameter τ, the maximum dimensionless deflection v_1^* obtained by the model $C1$ coincides with the one obtained by the Eringen model v_E^* if the value of the participation factor reported in Table 5 is used.

If the participation factor is negative the coupled model $C1$ is stiffer than the gradient elasticity model. Denoting by α_τ the par-

Table 5
Values of the participation factor for a simply supported nanobeam under a parabolic distributed load such that $v_1^* \equiv v_E^*$.

Dimensionless nonlocal parameter τ	Participation factor α	Dimensionless maximum deflection $v_1^* \equiv v_E^*$
0.1	1.7265	0.0116319
0.2	1.52145	0.0147569
0.3	1.40911	0.0199653
0.4	1.35081	0.0272569
0.5	1.31853	0.0366319

Table 6
Simply supported nanobeam under a parabolic distributed load: upper and lower bounds of the dimensionless maximum deflection and values (if any) of the participation factor such that the maximum deflection is vanishing.

Dimensionless nonlocal parameter τ	Coupled Model	Upper bound	Lower bound	Participation factor α_0
0.1	C1	$+\infty$	$-\infty$	−10.1291
	C2	0.011632	0.009167	–
	C3	0.009375	0.009167	–
0.2	C1	$+\infty$	$-\infty$	−2.51882
	C2	0.01475	0.01167	–
	C3	0.0125	0.01167	–
0.3	C1	$+\infty$	$-\infty$	−1.11604
	C2	0.01996	0.01583	–
	C3	0.01771	0.01583	–
0.4	C1	$+\infty$	$-\infty$	−0.626759
	C2	0.02725	0.02167	–
	C3	0.025	0.02167	–
0.5	C1	$+\infty$	$-\infty$	−0.400766
	C2	0.03663	0.02917	–
	C3	0.034375	0.02917	–

FIG. 1

The final version of this manuscript is available in COMPOSITES. PART B, ENGINEERING. doi.org/10.1016/j.compstruct.2015.03.033

FIG. 2

ticipation factor reported in Table 5 for a given τ, if α belongs to the interval $[0, \alpha_\tau]$ the model $C1$ is less stiff than the gradient elasticity model but it is stiffer than the Eringen model. For increasing values of α, i.e. for $\alpha > \alpha_\tau$, the model $C1$ becomes less stiff than the Eringen model.

Models $C2$ and $C3$ are less stiff than the local model for any value of α and τ. Further Fig. 1 shows that the maximum dimensionless deflection of the models $C2$ and $C3$ decreases with increasing α and τ with respect to the EM. Hence the models $C2$ and $C3$ are stiffer than the EM.

On the contrary the model $C1$ can be stiffer or not than the local model, the EM and the GM depending on the value of the participation factor.

Fig. 1 displays that the maximum dimensionless deflection of the simply supported nanobeam for the model $C1$ can become negative for some values of the parameters α and τ.

For the considered values of τ, the maximum dimensionless deflections of the models $C2$ and $C3$ belong to the strip defined by the upper and lower bounds reported in Table 6.

The maximum dimensionless deflection of the model $C1$ is positive if the participation factor is greater than the value α_0 reported in Table 6 for the corresponding parameter τ. If the participation factor is less than the value α_0 the maximum dimensionless deflection is negative due to the presence of an effective load, linearly depending on α, having an opposite sign with respect to the applied load.

- The maximum dimensionless deflections v_1^*, v_2^* and v_3^* of the models $C1$, $C2$ and $C3$ for a clamped nanobeam subjected to a parabolic distributed load is plotted in Fig. 2 for different values of the dimensionless length-scale parameter $\tau \in \{0, 0.1, 0.2, 0.3, 0.4, 0.5\}$. The participation factor α ranges in the interval $[-1, 2]$.

Setting $\alpha = 0$, the maximum dimensionless deflections obtained by the coupled models $C2$ and $C3$ coincide to the ones evaluated by the Eringen model (EM). In addition, for $\alpha = 0$, the dimensionless maximum deflections obtained by the model $C1$ coincides with the one calculated by the gradient elasticity model (GM). For $\alpha = 1$ the dimensionless maximum deflections obtained by models $C1$ and $C2$ coincide. For $\tau = 0$ the nonlocal models degenerate to the local (L) one.

The gradient elasticity model turns out to be stiffer than both local and Eringen models. For a given τ, the coupled models $C2$ and $C3$ are stiffer than the EM.

For a given dimensionless scale parameter τ, the maximum dimensionless deflection v_1^* obtained by model $C1$ coincides with the one achieved by the Eringen model if the value of the participation factor reported in Table 7 is used.

If the participation factor is negative the coupled model $C1$ is stiffer than the gradient elasticity model. Denoting by α_τ the participation factor reported in Table 7 for a given τ, if α belongs to the interval $[0, \alpha_\tau]$ the model $C1$ is less stiff than the gradient elasticity model but it is stiffer than the Eringen model. For increasing values of α, i.e. for $\alpha > \alpha_\tau$, the model $C1$ becomes less stiff than the Eringen model.

Table 7
Values of the participation factor for a clamped nanobeam under a parabolic distributed load such that $v_1^* = v_E^*$.

Dimensionless nonlocal parameter τ	Participation factor α	Dimensionless maximum deflection $v_1^* = v_E^*$
0.1	5.82277	0.00246528
0.2	6.96791	0.00309028
0.3	8.95565	0.00413194
0.4	11.7512	0.00559028
0.5	15.3491	0.00746528

Table 8
Clamped nanobeam under a parabolic distributed load: upper and lower bounds of the dimensionless maximum deflection and values (if any) of the participation factor such that the maximum deflection is vanishing.

Dimensionless nonlocal parameter τ	Coupled Model	Upper bound	Lower bound	Participation factor α_0
0.1	C1	$+\infty$	$-\infty$	−10.8573
	C2	0.002465	0	–
	C3	0.002465	0.00020833	–
0.2	C1	$+\infty$	$-\infty$	−2.71534
	C2	0.003090	0	–
	C3	0.003090	0.0008333	–
0.3	C1	$+\infty$	$-\infty$	−1.20692
	C2	0.004132	0	–
	C3	0.004132	0.001875	–
0.4	C1	$+\infty$	$-\infty$	−0.678915
	C2	0.005590	0	–
	C3	0.005590	0.003333	–
0.5	C1	$+\infty$	$-\infty$	−0.434512
	C2	0.007465	0	–
	C3	0.007465	0.00520833	–

The final version of this manuscript is available in COMPOSITES. PART B, ENGINEERING. doi.org/10.1016/j.compstruct.2015.03.033

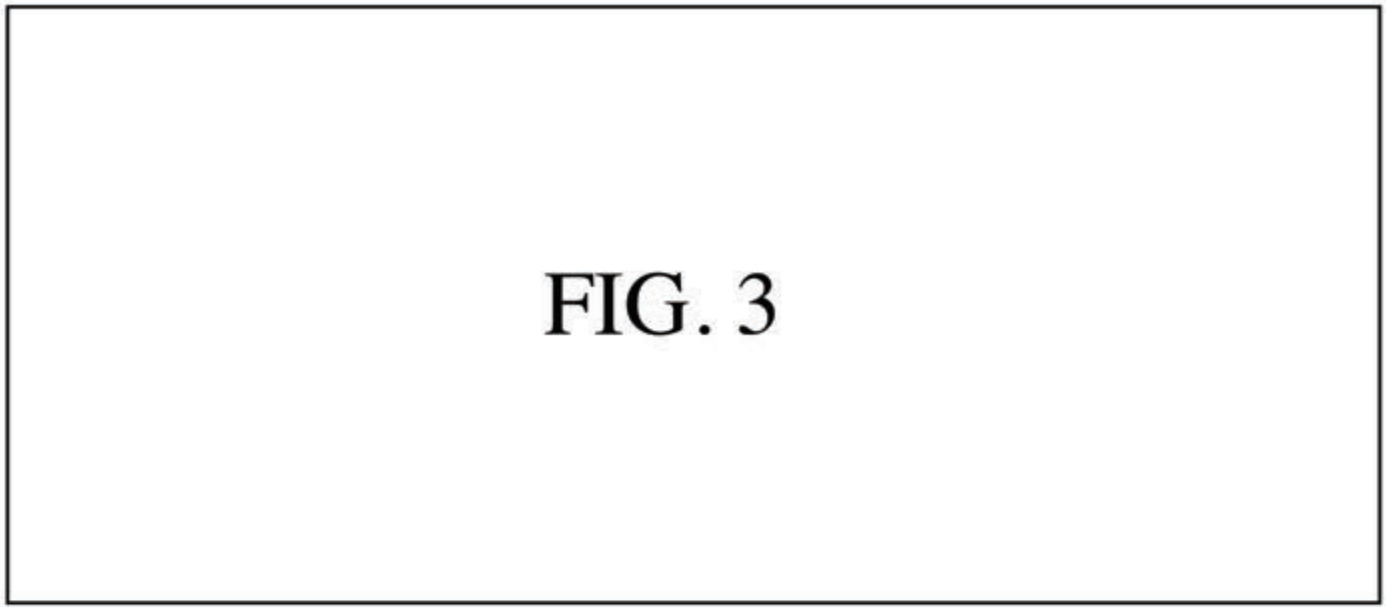

Hence, for a given τ, the coupled model $C1$ can be stiffer or not than the local model, EM and GM depending on the value of the participation factor.

Fig. 2 displays that the deflection of the midpoint of the clamped nanobeam for the model $C1$ can become negative for some values of the parameters α and τ.

For the considered values of τ, the maximum dimensionless deflections of the models $C2$ and $C3$ belong to the strip defined by the upper and lower bounds reported in Table 8. The maximum dimensionless deflection of the model $C1$ is positive if the participation factor is greater than the value α_0 reported in Table 8 for the corresponding parameter τ.

- The maximum dimensionless deflections v_1^*, v_2^* and v_3^* of the models $C1$, $C2$ and $C3$ for a nanocantilever under a linearly distributed load is plotted in Fig. 3 for different values of the dimensionless length-scale parameter $\tau \in \{0,0.1,0.2,0.3,0.4,0.5\}$ where the participation factor α ranges in the interval $[-1,2]$.

The maximum dimensionless deflections of the coupled models are plotted together with the deflections supplied by the local model, the Eringen model and the gradient elasticity model for comparison.

According to the results reported in Table 3, setting $\alpha = 0$, the maximum dimensionless deflection obtained by the model $C2$ for a given τ coincides to the one obtained by the model $C3$ and, in addition, coincides to the one evaluated by the Eringen model (EM). Moreover, the maximum dimensionless deflection obtained by the model $C1$, with $\alpha = 0$, for a given τ coincides with the corresponding one calculated by the gradient elasticity model (GM). Setting $\alpha = 1$ the dimensionless maximum deflection obtained by models $C1$ and $C2$, for a given τ, has the same value.

Note that the nonlocal models collapse to the local one (L) for $\tau = 0$ and the deflection is evidently independent of α.

Fig. 3 shows that the Eringen model, the gradient elasticity method and the coupled models $C2$ and $C3$ are stiffer than the local model for any value of τ and α. On the contrary the model $C1$ can be stiffer or not than the local model depending on the value of the participation factor.

For a given dimensionless length-scale parameter τ, the maximum dimensionless deflection v_1^* of the nanocantilever under a linearly distributed load obtained by model $C1$ coincides to the one obtained by the Eringen model v_E^* if the value of the participation factor reported in Table 9 is used.

Table 9
Nanocantilever under a linearly distributed load: values of the participation factor such that $v_1^* \equiv v_E^*$.

Dimensionless nonlocal parameter τ	Participation factor α	Dimensionless maximum deflection $v_1^* \equiv v_E^*$
0.1	0.641379	0.03
0.2	0.780003	0.02
0.3	0.908042	0.003333
0.4	1.01061	−0.02
0.5	1.0867	−0.05

Table 10
Nanocantilever under a linearly distributed load: upper and lower bounds of the dimensionless maximum deflection and values (if any) of the participation factor such that the maximum deflection is vanishing.

Dimensionless nonlocal parameter τ	Coupled Model	Upper bound	Lower bound	Participation factor α_0
0.1	C1	$+\infty$	$-\infty$	9.8627
	C2	0.03	0.01833	–
	C3	0.03	0.0175	–
0.2	C1	$+\infty$	$-\infty$	2.3975
	C2	0.02	0.010833	–
	C3	0.02	0.075	–
0.3	C1	$+\infty$	$-\infty$	1.03418
	C2	−0.001667	0.00333	1.46517
	C3	−0.009167	0.00333	0.619921
0.4	C1	$+\infty$	$-\infty$	0.567208
	C2	−0.01917	−0.02	–
	C3	−0.02	−0.0325	–
0.5	C1	$+\infty$	$-\infty$	0.356056
	C2	−0.04167	−0.05	–
	C3	−0.05	−0.0625	–

In the case of a negative participation factor, the coupled model $C1$ is less stiff than the gradient elasticity model and of the classical (local) method. Denoting by α_τ the participation factor reported in Table 9 for a given τ, if α belongs to the interval $[0, \alpha_\tau]$ the model $C1$ is stiffer than the gradient elastic model but it is less stiff than the Eringen model. For increasing values of α, i.e. for $\alpha > \alpha_\tau$, the model $C1$ becomes stiffer than the Eringen model.

Fig. 3 shows that the deflection of the nanocantilever tip can become negative (i.e. the nanocantilever tip moves in the opposite

The final version of this manuscript is available in COMPOSITES. PART B, ENGINEERING. doi.org/10.1016/j.compstruct.2015.03.033

direction of the applied load) for given values of the parameters α and τ.

On the basis of the results reported in Section 4.3, the upper and lower bounds of the maximum dimensionless deflection of the coupled models for $\alpha \to +\infty$ and $\alpha \to 0$ (models $C2$ and $C3$) or $\alpha \to -\infty$ (models $C1$) together with the values (if any) of the participation factor such that the tip deflection is vanishing are reported in Table 10 for the considered τ.

The linearity of the plot in Fig. 3 associated with the model $C1$ shows that, for any τ value, there is a participation factor α_0 (reported in Table 10) such that the maximum dimensionless deflection of the nanocantilever is vanishing. Therefore all the considered values of τ can be used for the model $C1$.

Both models $C2$ and $C3$ are stiffer than the EM and the gap in terms of the maximum dimensionless deflection between the models $C2$ and $C3$ increases for increasing α and τ. Conversely, the model $C1$ becomes stiffer or less stiff than EM and GM depending on the participation factor α.

6. Conclusion

The main contributions provided in the present manuscript are summarized as follows:

- new nonlocal models of functionally graded Bernoulli–Euler nanobeams have been formulated by a variational approach. The nonlocal treatment is based on two parameters, i.e. length-scale parameter and participation factor, which are suitable to modify the displacement solution fields associated with the Eringen and gradient elasticity theories;
- exact solutions have been established for statically determinate and indeterminate nanobeams providing thus new benchmarks for numerical analyses;
- Eringen nonlocal elasticity theory (EM) and gradient elasticity model (GM) have been recovered as special cases.

Acknowledgement

The study presented in this paper has been developed within the activities of the research program FARO 2012 – Compagnia San Paolo, Polo delle Scienze e delle Tecnologie, University of Naples Federico II – and of the DPC/ReLUIS2014-AQDPC/ReLUIS2014-2016 project (theme: reinforced concrete structures) funded by the Italian Department of Civil Protection.

Appendix A

The integration by parts of the last two integrals into Eq. (5) yields

$$\begin{aligned}\int_0^L M_1 \dot{\nu}^{(3)} dx &= M_1 \dot{\nu}^{(2)}\big|_{x=0,L} - \int_0^L M_1^{(1)} \dot{\nu}^{(2)} dx \\ \int_0^L M^{(3)} \dot{\nu}^{(3)} dx &= M^{(3)} \dot{\nu}^{(2)}\Big|_{x=0,L} - \int_0^L M^{(4)} \dot{\nu}^{(2)} dx\end{aligned} \tag{A.1}$$

so that we have

$$\begin{aligned}&\int_0^L M_1 \dot{\nu}^{(3)} dx \begin{bmatrix} c^2 \\ \alpha^2 c^2 \\ \alpha^2 c^2 \end{bmatrix} + \int_0^L M^{(3)} \dot{\nu}^{(3)} dx \begin{bmatrix} 0 \\ 0 \\ \alpha^2 c^4 \end{bmatrix} = \\ &- \int_0^L M_1^{(1)} \dot{\nu}^{(2)} dx \begin{bmatrix} c^2 \\ \alpha^2 c^2 \\ \alpha^2 c^2 \end{bmatrix} - \int_0^L M^{(4)} \dot{\nu}^{(2)} dx \begin{bmatrix} 0 \\ 0 \\ \alpha^2 c^4 \end{bmatrix} \\ &+ \left(M_1 \begin{bmatrix} c^2 \\ \alpha^2 c^2 \\ \alpha^2 c^2 \end{bmatrix} + M^{(3)} \begin{bmatrix} 0 \\ 0 \\ \alpha^2 c^4 \end{bmatrix} \right) \dot{\nu}^{(2)}\Big|_{x=\{0,L\}}\end{aligned} \tag{A.2}$$

The boundary terms in Eq. (A.2) vanish due to the static boundary conditions associated with $\nu^{(2)}$ reported in Table 1 so that we have

$$\begin{aligned}&\int_0^L M_1 \dot{\nu}^{(3)} dx \begin{bmatrix} c^2 \\ \alpha^2 c^2 \\ \alpha^2 c^2 \end{bmatrix} + \int_0^L M^{(3)} \dot{\nu}^{(3)} dx \begin{bmatrix} 0 \\ 0 \\ \alpha^2 c^4 \end{bmatrix} \\ &= - \int_0^L M_1^{(1)} \dot{\nu}^{(2)} dx \begin{bmatrix} c^2 \\ \alpha^2 c^2 \\ \alpha^2 c^2 \end{bmatrix} - \int_0^L M^{(4)} \dot{\nu}^{(2)} dx \begin{bmatrix} 0 \\ 0 \\ \alpha^2 c^4 \end{bmatrix}.\end{aligned} \tag{A.3}$$

References

[1] Aydogdu M. A general nonlocal beam theory: its application to nanobeam bending, buckling and vibration. Phys E 2009;41:1651–5.
[2] Asghari M, Kahrobaiyan MH, Ahmadian MT. A nonlinear Timoshenko beam formulation based on the modified couple stress theory. Int J Eng Sci 2010;48:1749–61.
[3] Aydogdu M, Filiz S. Modeling carbon nanotube-based mass sensors using axial vibration and nonlocal elasticity. Phys E 2011;43:1229–34.
[4] Asghari M, Kahrobaiyan MH, Nikfar M, Ahmadian MT. A size-dependent nonlinear Timoshenko microbeam model based on the strain gradient theory. Acta Mech 2012;223:1233–49.
[5] Thai HT. A nonlocal beam theory for bending, buckling, and vibration of nanobeams. Int J Eng Sci 2012;52:56–64.
[6] Ansari R, Mirnezhad M, Sahmani S. An accurate molecular mechanics model for computation of size-dependent elastic properties of armchair and zigzag single-walled carbon nanotubes. Meccanica 2013;48:1355–67.
[7] Ansari R, Gholami R, Faghih Shojaei M, Mohammadi V, Sahmani S. Size-dependent bending, buckling and free vibration of functionally graded Timoshenko microbeams based on the most general strain gradient theory. Compos Struct 2013;100:385–97.
[8] Akgöz B, Civalek Ö. A size-dependent shear deformation beam model based on the strain gradient elasticity theory. Int J Eng Sci 2013;70:1–14.
[9] Brcic M, Canadija M, Brnic J. Estimation of material properties of nanocomposite structures. Meccanica 2013;48:2209–22.
[10] Canadija M, Brcic M, Brnic J. A finite element model for thermal dilatation of carbon nanotubes. Rev Adv Mater Sci 2013;33:1–6.
[11] Kiani K. Characterization of free vibration of elastically supported double-walled carbon nanotubes subjected to a longitudinally varying magnetic field. Acta Mech 2013;224:3139–51.
[12] Kiani K. Axial buckling analysis of vertically aligned ensembles of single-walled carbon nanotubes using nonlocal discrete and continuous models. Acta Mech 2014;225:3569–89.
[13] Peerlings RHJ, de Borst R, Brekelmans WAM, de Vree JHP. Gradient enhanced damage for quasi brittle materials. Int J Numer Meth Eng 1996;39:3391–403.
[14] Pijaudier-Cabot G, Bažant ZP. Nonlocal damage theory. ASCE J Eng Mech 1987;113:1512–33.
[15] Fleck NA, Hutchinson JW. A reformulation of strain gradient plasticity. J Mech Phys Solids 2001;49:2245–71.
[16] Peerlings RHJ, Geers MGD, de Borst R, Brekelmans WAM. A critical comparison of nonlocal and gradient-enhanced softening continua. Int J Solids Struct 2001;38:7723–46.
[17] Abu Al-Rub RK, Voyiadjis GZ. Analytical and experimental determination of the material intrinsic length scale of strain gradient plasticity theory from micro- and nanoindentation experiments. Int J Plast 2004;20:1139–82.
[18] Marotti de Sciarra F. On non-local and non-homogeneous elastic continua. Int J Solids Struct 2009;46(3):651–76.
[19] Marotti de Sciarra F. A general theory for nonlocal softening plasticity of integral-type. Int J Plast 2008;24:1411–39.
[20] Marotti de Sciarra F. Novel variational formulations for nonlocal plasticity. Int J Plast 2009;25:302–31.
[21] Marotti de Sciarra F. Variational formulations, convergence and stability properties in nonlocal elastoplasticity. Int J Solids Struct 2008;45:2322–54.
[22] Voyiadjis GZ, Pekmezi G, Deliktas B. Nonlocal gradient-dependent modeling of plasticity with anisotropic hardening. Int J Plast 2010;26:1335–56.
[23] Eringen AC. Nonlocal continuum field theories. New York: Springer-Verlag; 2002.
[24] Eringen AC. Theory of nonlocal elasticity and some applications. Res Mech 1987;21:313–42.
[25] Peddieson J, Buchanan R, McNitt RP. Application of nonlocal continuum models to nanotechnology. Int J Eng Sci 2003;41:305–12.
[26] Luciano R, Willis JR. Boundary-layer corrections for stress and strain fields in randomly heterogeneous materials. J Mech Phys Solids 2003;51:1075–88.
[27] Luciano R, Willis JR. Hashin–Shtrikman based FE analysis of the elastic behaviour of finite random composite bodies. Int J Fract 2006;137:261–73.
[28] Park SK, Gao XL. Bernoulli–Euler beam model based on a modified couple stress theory. J Micromech Microeng 2006;16:2355–9.
[29] Giannakopoulos AE, Stamoulis K. Structural analysis of gradient elastic components. Int J Solids Struct 2007;44:3440–51.

The final version of this manuscript is available in COMPOSITES. PART B, ENGINEERING. doi.org/10.1016/j.compstruct.2015.03.033

[30] Reddy JN. Nonlocal theories for bending, buckling and vibration of beams. Int J Eng Sci 2007;45:288–307.
[31] Wang Q, Liew KM. Application of nonlocal continuum mechanics to static analysis of micro- and nano-structures. Phys Lett A 2007;363:236–42.
[32] Barretta R, Marotti de Sciarra F, Diaco M. Small-scale effects in nanorods. Acta Mech 2014;225:1945–53.
[33] Barretta R, Marotti de Sciarra F. Analogies between nonlocal and local Bernoulli–Euler nanobeams. Arch Appl Mech 2015;85(1):89–99.
[34] Akgöz B, Civalek Ö. Analysis of micro-sized beams for various boundary conditions based on the strain gradient elasticity theory. Arch Appl Mech 2012;82:423–43.
[35] Eltaher MA, Emam SA, Mahmoud FF. Static and stability analysis of nonlocal functionally graded nanobeams. Compos Struct 2013;96:82–8.
[36] Aifantis EC. Update on a class of gradient theories. Mech Mater 2003;35:259–80.
[37] Timoshenko SP, Gere JM. Theory of elastic stability. New York: McGraw-Hill; 1961.
[38] Roque CMC, Fidalgo DS, Ferreira AJM, Reddy JN. A study of a microstructure dependent composite laminated Timoshenko beam using a modified couple stress theory and a meshless method. Compos Struct 2013;96:532–7.
[39] Simsek M, Kocatürk T, Akbas SD. Static bending of a functionally graded microscale Timoshenko beam based on the modified couple stress theory. Compos Struct 2013;95:740–7.
[40] Ma HM, Gao XL, Reddy JN. A microstructure-dependent Timoshenko beam model based on a modified couple stress theory. J Mech Phys Solids 2008;56:3379–91.
[41] Reddy JN. Nonlocal nonlinear formulations for bending of classical and shear deformation theories of beams and plates. Int J Eng Sci 2010;48:1507–18.
[42] Wang B, Zhao J, Zhou S. A micro scale Timoshenko beam model based on strain gradient elasticity theory. Eur J Mech A/Solids 2010;29:591–9.
[43] Marotti de Sciarra F, Barretta R. A gradient model for Timoshenko nanobeams. Phys E 2014;62:1–9.
[44] Apuzzo A, Barretta R, Luciano R. Some analytical solutions of functionally graded Kirchhoff plates. Compos B 2015;68:266–9.
[45] **Barretta R, Luciano R. Exact solutions of isotropic viscoelastic functionally graded Kirchhoff plates. Compos Struct 2014;118:448–54.** http://dx.doi.org/10.1007/s00161-014-0385-2.
[46] Barretta R, Luciano R. Analogies between Kirchhoff plates and functionally graded Saint-Venant beams under torsion. Cont Mech Thermodyn 2015;27(3):499–505.
[47] Barretta R, Feo L, Luciano R. Some closed-form solutions of functionally graded beams undergoing nonuniform torsion. Compos Struct 2015;123:132–6.
[48] Barretta R, Feo L, Luciano R. Torsion of functionally graded nonlocal viscoelastic circular nanobeams. Compos B 2015;72:217–22.
[49] Ferreira AJM. Thick composite beam analysis using a global meshless approximation based on radial basis functions. Mech Adv Mater Struct 2003;10(3):271–84.
[50] Mazzucco G, Salomoni VA, Majorana CE. Three-dimensional contact-damage coupled modelling of FRP reinforcements – Simulation of delamination and long-term processes. Comput Struct 2012;110–111:15–31.
[51] Caporale A, Feo L, Luciano R, Penna R. Numerical collapse load of multi-span masonry arch structures with FRP reinforcement. Compos B 2013;54(1):71–84.
[52] Feo L, Mosallam AS, Penna R. Mechanical behavior of web-flange junctions of thin-walled pultruded I-profiles: an experimental and numerical evaluation. Compos B 2013;48:18–39.
[53] Ghannadpour SAM, Mohammadi B, Fazilati J. Bending, buckling and vibration problems of nonlocal Euler beams using Ritz method. Compos Struct 2013;96:584–9.
[54] Giunta G, Metla N, Belouettar S, Ferreira AJM, Carrera E. A thermo-mechanical analysis of isotropic and composite beams via collocation with radial basis functions. J Therm Stresses 2013;36(11):1169–99.
[55] Mancusi G, Feo L. A refined finite element formulation for the microstructure-dependent analysis of two-dimensional (2D) lattice materials. Materials 2013;6:1–17.
[56] Cricrì G, Luciano R. Homogenised properties of composite materials in large deformations. Compos Struct 2013;103:9–17.
[57] **Marotti de Sciarra F. A nonlocal finite element approach to nanobeams. Adv Mech Eng 2013:1–8.** http://dx.doi.org/10.1155/2013/720406 **[ID 720406].**
[58] Thai CH, Ferreira AJM, Carrera E, Nguyen-Xuan H. Isogeometric analysis of laminated composite and sandwich plates using a layerwise deformation theory. Compos Struct 2013;104:196–214.
[59] Bruno D, Greco F, Luciano R, Nevone Blasi P. Nonlinear homogenized properties of defected composite materials. Comput Struct 2014;134:102–11.
[60] Caporale A, Feo L, Luciano R. Damage mechanics of cement concrete modeled as a four-phase composite. Compos B 2014;65:124–30.
[61] Caporale A, Feo L, Hui D, Luciano R. Debonding of FRP in multi-span masonry arch structures via limit analysis. Compos Struct 2014;108(1):856–65.
[62] Marotti de Sciarra F. Finite element modelling of nonlocal beams. Phys E 2014;59:144–9.
[63] Feo L, Greco F, Leonetti L, Luciano R. Mixed-mode fracture in lightweight aggregate concrete by using a moving mesh approach within a multiscale framework. Compos Struct 2015;123:88–97.
[64] Ma HM, Gao XL, Reddy JN. A microstructure-dependent Timoshenko beam model based on a modified couple stress theory. J Mech Phys Solids 2008;56:3379–91.
[65] Voyiadjis GZ, Abu Al-Rub RK, Palazotto AN. Thermodynamic framework for coupling of non-local viscoplasticity and non-local anisotropic viscodamage for dynamic localization problems using gradient theory. Int J Plast 2004;20:981–1038.
[66] Eringen AC. On differential equations of nonlocal elasticity and solutions of screw dislocation and surface waves. J Appl Phys 1983;54:4703–10.
[67] Lemaitre J, Chaboche JL. Mechanics of solids materials. Cambridge, UK: Cambridge University Press; 1994.
[68] Wang Q. Wave propagation in carbon nanotubes via nonlocal continuum mechanics. J Appl Phys 2005;98:124301.

The final version of this manuscript is available in COMPOSITES. PART B, ENGINEERING. doi.org/10.1016/j.compstruct.2015.03.033

FIGURES

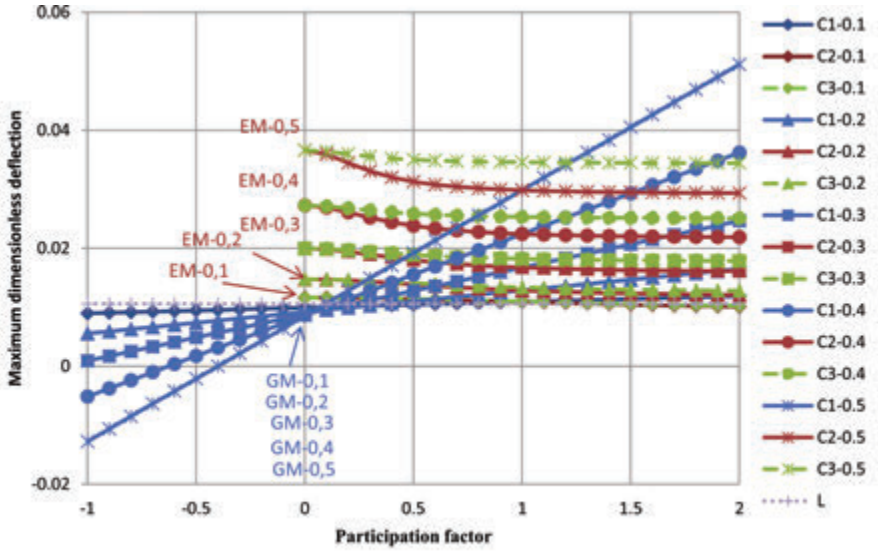

Fig. 1. Maximum dimensionless displacements of a simply supported nanobeam under a parabolic distributed load.

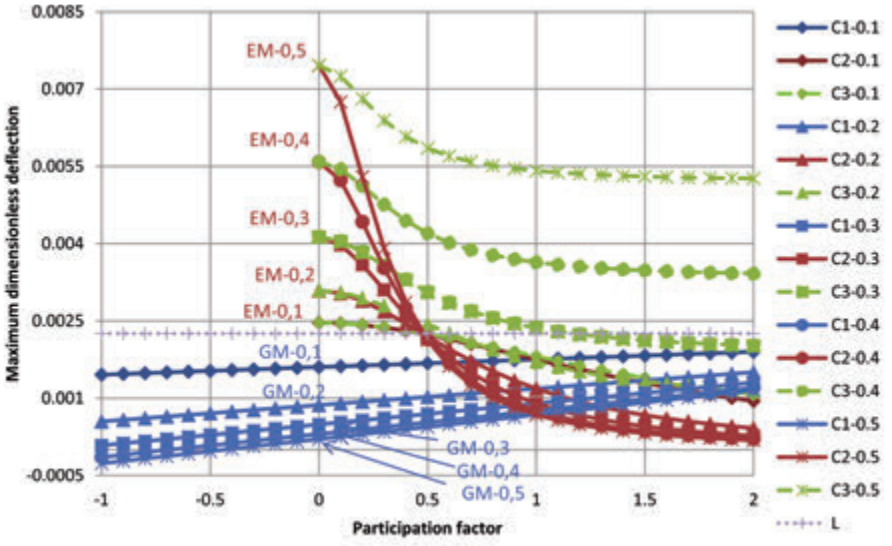

Fig. 2. Maximum dimensionless displacements of a clamped nanobeam under a parabolic distributed load.

FIGURES

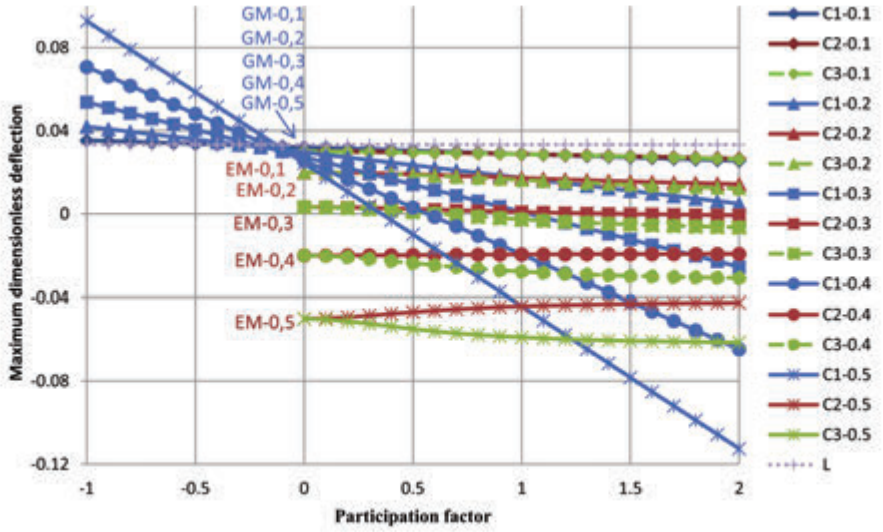

Fig. 3. Maximum dimensionless displacements of a nanocantilever under a linearly distributed load.